CATALYTIC MECHANISM OF NITRILE HYDRATASE PROPOSED BY TIME-RESOLVED X-RAY CRYSTALLOGRAPHY USING A NOVEL SUBSTRATE, *tert*-BUTYLISONITRILE*

Koichi Hashimoto,[1] Hiroyuki Suzuki,[2] Kayoko Taniguchi,[3] Takumi Noguchi,[2] Masafumi Yohda,[1] and Masafumi Odaka[2]

from [‡]Department of Biotechnology and Life Science, Graduate School of Technology, Tokyo University of Agriculture and Technology, 2-24-16 Naka-cho, Koganei, Tokyo 184-8588, Japan, [2]Institute of Materials Science, University of Tsukuba, Tsukuba 305-8573, and [3] Eco-Soft Material Research Units, RIKEN, Wako, Saitama 351-0198, Japan

Running Title: Catalytic mechanism of nitrile hydratase

Address correspondence to: Masafumi Odaka, Department of Biotechnology and Life Science, Graduate School of Technology, Tokyo University of Agriculture and Technology, 2-24-16 Naka-cho, Koganei, Tokyo 184-8588, Japan; Tel / Fax: +81-42-388-7479; E-mail: modaka@cc.tuat.ac.jp

Nitrile hydratases (NHases) have an unusual iron or cobalt catalytic center with two oxidized cysteine ligands, cysteine-sulfinic acid (Cys-SO_2H) and -sulfenic acid (Cys-SOH), catalyzing the hydration of nitriles to amides. Recently, we found that the NHase of *Rhodococcus erythropolis* N771 exhibited an additional catalytic activity, converting *tert*-butylisonitrile (*t*BuNC) to *tert*-butylamine. Taking advantage of the slow reactivity of *t*BuNC and the photoreactivity of nitrosylated NHase, we present the first structural evidence for the catalytic mechanism of NHase with time-resolved X-ray crystallography. By monitoring the reaction with ATR-FTIR spectroscopy, the product from the isonitrile carbon was identified as a CO molecule. Crystals of nitrosylated inactive NHase were soaked with *t*BuNC. The catalytic reaction was initiated by photo-induced denitrosylation and stopped by flash-cooling. *t*BuNC was first trapped at the hydrophobic pocket above the Fe center and then coordinated to the Fe ion at 120 min. At 440 min, the electron density of *t*BuNC was significantly altered, and a new electron density was observed near the isonitrile carbon as well as the sulfenate oxygen of αCys114. These results demonstrate that the substrate was coordinated to the iron and then attacked by a solvent molecule activated by αCys114-SOH.

Nitrile hydratases (NHase) catalyze the hydration of nitriles to the corresponding amides and are used as catalysts in the production of acrylamide, making them one of the most important industrial enzymes (1,2). NHases contain a non-heme Fe^{3+} or non-corrin Co^{3+}

catalytic center. Fe-type NHases show unique photoreactivity: the enzyme is inactivated by nitrosylation in the dark and immediately re-activated by photo-induced denitrosylation (3-5). The protein structure is highly conserved among all known NHases (6-9) as well as a related enzyme, thiocyanate hydrolase (10). The metal site is also conserved, with a distorted octahedral geometry. All ligand residues are involved in a strictly conserved motif of the α subunit, Cys1-Xxx-Leu-Cys2-Ser-Cys3, where two amide nitrogens of Ser and Cys3 and three Cys sulfurs are coordinated to the metal (6). Cys2 and Cys3 are post-translationally modified to cysteine-sulfinic acid (Cys-SO_2H) and -sulfenic acid (Cys-SOH), respectively (7), which probably take deprotonated forms at the metal site (11). The sixth ligand site is occupied by a solvent molecule (8), or by a nitric oxide (NO) molecule in nitrosylated Fe-type NHase (7).

Several reaction mechanisms have been proposed based on the protein structures (1,6). First, nitriles directly bind to the metal to facilitate the nucleophilic attack of a water molecule on the nitrile carbon. In the other mechanisms, a water molecule activated by the metal directly or indirectly attacks nitriles trapped near the metal. In all cases, the metal is suspected to function as a Lewis acid. By reconstituting Fe-type NHase from recombinant unmodified subunits, we demonstrated that the post-translational modifications of its cysteine ligands are essential for its catalytic activity (12). We also found that specific oxidation of the Cys-SOH ligand to Cys-SO_2H resulted in irreversible inactivation (13). Kovacs and her colleagues studied the ligand exchange reaction in the low-spin Co^{3+}-containing NHase model complexes and concluded that the trans-thiolate sulfur played an important role in promoting the ligand exchange at the sixth site (14). Later, by using a sulfenate-ligated Fe complex, they showed that protonation/deprotonation states of the sulfenate oxygen were modulated by the unmodified Cys thiolate ligand (15). An N_3S_2-type model complex, $[Co(PyPS)(H_2O)]^-$, slowly hydrolyzes nitriles (18 turnovers in 4 h) (16). Interestingly, the hydration activity was enhanced by the mono-oxygenation of one of two sulfur ligands (17). Heinrich *et al*. demonstrated that $Na[Co(L\text{-}N_2SOSO)(t\text{BuNC})_2]$ exhibited the nitrile hydration activity but that $(Me_4N)[Co(L\text{-}N_2SO_2SO_2)(t\text{BuNC})_2]$ did not (18). These results indicate that the oxidized cysteine ligands, especially the Cys-SOH ligand, play an important role in the catalysis. Recently, theoretical calculations, including density functional calculations (19,20) as well as molecular dynamics simulations (21), have been applied to the mechanisms described above. However, the detailed mechanism remains unclear because of a lack of direct information on the reaction intermediates.

We recently found that an Fe-type NHase from *Rhodococcus erythropolis* N771 (*Re*NHase) catalyzes the conversion of isonitriles to the corresponding amines (22). Although the other

product derived from the isonitrile carbon was not identified, the kinetic analyses revealed that the K_m for *tert*-butylisonitrile (*t*BuNC) was comparable to that for methacrylonitrile, while k_{cat} (1.8×10^{-2} s^{-1}) was 1.8×10^5 times smaller. In this study, taking advantage of the slow reactivity of *t*BuNC as well as the photo-reactivity of nitrosylated inactive *Re*NHase (3,4), we obtained structural evidence on the reaction mechanism by studying the time course of the *t*BuNC catalysis with X-ray crystallography. Based on the results, we propose a reaction mechanism in which the sulfenate group of αCys114-SO^- plays a key role in the catalysis.

EXPERIMENTAL PROCEDURES

Materials- Nitrile hydratase from *Rhodococcus erythropolis* N771 (*Re*NHase) was inactivated by endogenous NO molecules in living cells in the dark (4, 23). *Re*NHase was purified in the nitrosylated form in the dark as described previously (23). The purified nitrosylated *Re*NHase was stored in 50 mM Tris-HCl, pH 7.5, at -80˚C in the dark at a concentration of 20 mg/mL. The concentration of the nitrosylated NHase was determined by measuring the absorbance at 280 nm (ε_{280} = 1.7 $mL\cdot mg^{-1}\cdot cm^{-1}$). *tert*-butylisonitirle (*t*BuNC) was purchased from Tokyo Chemical Industry Co., Ltd. (Tokyo, Japan). All the other reagents used in this study were of the highest grade available.

ATR-FTIR (Attenuated total reflectance-Fourier transform-infrared) measurements- The nitrosylated *Re*NHase (70 mg/mL) in 50 mM sodium phosphate, pH 7.5, was loaded on the surface of a 3 reflection silicon prism (3 mm in diameter) in the ATR accessory (DuraSampl*IR* II, Smiths Detection, CT, USA) and dried under nitrogen gas flow. Subsequently, 1.5 μL of water ($H_2{}^{16}O$ or $H_2{}^{18}O$) was added to the sample. The sample space was sealed with a CaF_2 plate and a greased Teflon spacer (0.7 mm in thickness). The substrate, 0.5 μL of neat *t*BuNC, was also enclosed in this sealed space as a drop on the CaF_2 plate, to be supplied to the *Re*NHase solution as a vapor. The sample was stabilized at room temperature in the dark for four hours.

FTIR spectra were measured on a Bruker IFS-66/S spectrophotometer equipped with an MCT detector (D313-L). All spectra were recorded at 4 cm^{-1} resolution. A single-beam spectrum was recorded for 100 s before illumination, and ten spectra (100 s scans) were successively recorded after 10 s illumination by continuous white light from a halogen lamp (Hoya-Schott HL150; ~60 mW cm^{-2} at the sample). Light-induced difference spectra were calculated by subtracting the dark spectra from each spectrum after illumination. The baseline distortion was corrected by subtracting the corresponding spectra measured in the same manner but without illumination.

For CO detection, 6 μL of hemoglobin (50 mg/mL) in 50 mM Tris-HCl, pH 7.5, was lightly dried on a silicon ATR prism, and 6 μL of the

nitrosylated *Re*NHase sample (70 mg/mL) in Tris-HCl, pH 7.5, was placed beside the hemoglobin. The sample space was sealed with a CaF_2 plate, on which 0.5 μL of *t*BuNC was placed, and a greased Teflon spacer (Fig. 1). The *Re*NHase sample was photoactivated by white-light illumination for 1 min. FTIR spectra with 10 s scans were recorded at 0, 20, 30 and 60 min after illumination.

Crystallization of ReNHase- Crystals of the nitrosylated *Re*NHase were grown using the vapor diffusion hanging-drop method at 20˚C. Two microliters of the nitrosylated *Re*NHase (20 mg/mL protein in 50mM Tris-HCl, pH 7.5) was mixed with an equal amount of the precipitant solution (20% PEG8000, 0.10 M Tris-HCl, pH 7.5, 0.30 M $MgCl_2$) and equilibrated against 0.40 mL precipitant solution. Crystals with dimensions of about 0.4 × 0.3 × 0.3 mm^3 grew within a day in the dark at 20˚C. When crystals of the nitrosylated NHase were dissolved in 50 mM Tris-HCl, pH 7.5, the enzyme solution exhibited trace amounts of methacrylonitrile hydration activity in the dark, but it had a specific activity of 7.3×10^2 units/mg after light-induced denitrosylation (10,000 lx) with a cold light illumination system (LG-PS2, OLYMPUS, Japan) for 15 min.

Preparation of the ReNHase crystals without or with tBuNC- Crystals of the nitrosylated *Re*NHase were first vapor-soaked with cryoprotectant solution (30 % PEG8000, 0.10 M Tris/HCl, pH 7.5, 0.60 M $MgCl_2$) for one day by being swapped in mother liquor. They were then vapor-soaked for a day with mother liquor solution containing *t*BuNC at a final concentration of 0.10 M. After being mounted, *Re*NHases in the crystals were activated by light-induced denitrosylation (10,000 lx) with a cold light illumination system (LG-PS2, OLYMPUS, Japan), and the reaction proceeded for 18, 120, 340 and 440 min at 20˚C. At each elapsed time, the reaction was terminated by flash-cooling with N_2 gas at 95 K.

X-ray data collections, structure determinations and refinements- Diffraction data were collected using a Quantum 315 CCD detector (ADSC) at the beamline BL-5A (λ = 1.000 Å) of the Photon Factory (Tsukuba, Japan) at 95 K. Each data set was indexed, merged and scaled with the HKL2000 program suite (24). The *Re*NHase crystals belonged to the C2 space group. One hetero-dimer of α and β subunits populated the asymmetric unit. Molecular replacement was performed with MOLREP (25) in the CCP4 program suite (26) using the structure of the nitrosylated *Re*NHase in the $P2_12_12$ space group (Protein Data Bank: accession code 2ahj) (7) as the initial coordinates. The obtained models were improved by iterative cycles of crystallographic refinement using REFMAC5 (27) and manual model rebuilding using Coot (28). Models were cross-validated by the SigmaA-weighted electron

density maps (29) calculated with both $2mF_{obs}$-DF_{calc} and mF_{obs}-DF_{calc} coefficients. The refinements were performed using a maximum likelihood target with bulk solvent corrections. During the structure refinement, ~5% of the amplitude data were set aside to monitor the progress of refinement using the R_{free}-factor. Solvent water molecules were gradually introduced if the peaks that were contoured at more than 4.0 σ in the mF_{obs}-DF_{calc} electron density were in the range of a hydrogen bond. *tert*-butyl groups of *t*BuNC were fit on the resultant difference electron density map by handling, and their coordinate data were then refined using REFMAC5 (27). All structural figures were generated using PyMol (http://pymol.sourceforge.net/).

RESULTS AND DISCUSSION

Identification of the product from the isonitrile carbon by ATR-FTIR measurements.----To identify all products except for the amine, the reaction was monitored using ATR-FTIR. *t*BuNC was added as a vapor to nitrosylated NHase, and the enzyme was activated by light-induced denitrosylation. Several prominent positive peaks, all arising from *tert*-butylamine (*t*$BuNH_2$), increased their intensities as the reaction proceeded, whereas no signals from other origins were detected (Fig. 2). Supposing that the other product possessing a carbon atom was CO, which escaped from the solution as a gas, we attempted CO detection by trapping using hemoglobin. Hemoglobin was located on a silicon ATR crystal, and nitrosylated *Re*NHase solution and *t*BuNC were separately placed in a sealed space (Fig. 1). A CO molecule-bound hemoglobin was monitored by ATR-FTIR after light activation of *Re*NHase (Fig. 3). The CO-stretching signal of CO-hemoglobin was observed at 1953 cm^{-1}, and its intensity increased with the reaction time. The CO peak appeared at a downshifted frequency of 1908 cm^{-1} when the *Re*NHase reaction was performed in an $H_2{}^{18}O$ buffer, confirming that CO was produced by the *Re*NHase-consuming water. Thus, we concluded that *Re*NHase hydrolyzed *t*BuNC to produce *t*$BuNH_2$ and CO (*t*BuNC + H_2O → *t*$BuNH_2$ + CO).

Time-resolved X-ray crystallography of the reaction of ReNHase with tBuNC.----Crystals of nitrosylated *Re*NHase were soaked with *t*BuNC, and the reaction was started by light-induced denitrosylation at 293 K. At 18, 120, 340 and 440 min, the reaction was stopped by flash-cooling at 95 K, at which point the crystal structure was determined. Details of data collection and refinement statistics are summarized in Table 1. Unfortunately, we could not collect data from the crystals that were incubated longer because those crystals were damaged. The overall structure at each elapsed time was essentially unchanged except for the pocket above the Fe^{3+} center (Fig.

4). αCys112-SO_2^- (αCSD112) and αCys114-SO^- (αCSO114) modifications were clearly observed in all structures determined.

Before soaking with *t*BuNC, an NO molecule was observed at a distance of 2.1 Å from the Fe^{3+} (Fig. 4A). The Fe-N(NO) distance is 0.6 Å longer than observed in the previous structure (Protein Data Bank: accession code 2ahj) (7). In the previous structure, the NO was likely to be pushed toward Fe^{3+} by 1,4-dioxane, the co-precipitant used (7). After soaking with *t*BuNC, the electron density of *t*BuNC was clearly observed in the pocket (Fig. 4B) with the *tert*-butyl group facing the NO molecule coordinated to the Fe^{3+}. Because of the limited space in the hydrophobic pocket, the bulky *tert*-butyl group must face the iron in its nitrosylated state. In addition to the original conformation (conformer A), Sγ of βMet40 took another conformation (conformer B) with occupancies of A: B = 0.25: 0.75. Movement of Sγ of βMet40 to conformer B is likely due to the occupation of the hydrophobic pocket by *t*BuNC. We hypothesize that conformer B is less stable because of steric hindrance between Sγ and the amide oxygen of βMet40 (Fig. 5).

At 18 min, electron densities of NO and *t*BuNC, especially that of the isonitrile group, were attenuated (Fig. 4C). Sγ of βMet40 remained disordered, but the occupancy of conformer A increased to 0.55. At 120 min, the NO disappeared, and a *t*BuNC molecule was coordinated to Fe^{3+} with an Fe-C(-NC) length of 2.1 Å (Fig. 4D). βMet40 took conformer A again. The rotation of the *t*BuNC molecule could be driven by the recovery of βMet40 to conformer A.

The *Fo-Fc* electron density at 340 (supplemental Fig. S1) and 440 mins (Fig. 4E) were very similar to one another, but distinct from those observed at 120 min. In both structures, the *Fo-Fc* electron density corresponding to the *tert*-butyl group was moved about 1.0 Å away from the iron, and an extra electron density was observed near the isonitrile carbon as well as the sulfenate oxygen of αCys114. When the products, *t*$BuNH_2$ and CO, were included in the calculation of the electron density at 440 min, the refined model of *t*$BuNH_2$ was well fit on the *2Fo-Fc* electron density, but that of CO was not (supplemental Fig. S2). In addition, two positive electron densities were observed near the CO molecule in the *Fo-Fc* electron density. Alternatively, we calculated the electron density at 440 min by assuming the presence of only *t*$BuNH_2$. As shown in Fig. 4F, *t*$BuNH_2$ was well fit on the *2Fo-Fc* electron density, and two positive electron densities were observed above the Fe ion and near Oδ of the sulfenate group, in the *Fo-Fc* electron density. We assigned the positive densities as the carbon of the isonitrile group and the solvent water molecule (named as H_2Oa), respectively (Fig. 4F). All distances of Fe-C(-NC), C(-NC)-N(-NC), C(-NC)-O(H_2Oa), N(-NC)-O(H_2Oa) and O(H_2Oa)-O(-SO) converged at less than 2.2 Å (Table 2). The O(H_2Oa)-O(-SO) distance cannot

be explained. These atoms may be disordered because the occupancies of H_2Oa and Oδ of αCys114-SO^- converged on 0.50. Interestingly, a positive difference density was observed below Sγ of αCys114-SO^- in the *2Fo-Fc* electron density map after coordination of *t*BuNC (Fig. 4D-4F). The distance between the density and Sγ of αCys114-SO^- is 1.4 Å, and the angle Oδ(αCys114-SO^-)-Sγ(αCys114-SO^-)-the density was 133°. The positive density may represent an alternative position of Oδ of αCys114-SO^-.

Proposed catalytic mechanisms of NHase.----Based on the results, we propose the following catalytic mechanism: the *t*BuNC substrate binds the metal directly, and then a water molecule, activated by Oδ of αCys114-SO^-, makes a nucleophilic attack on the isonitrile carbon to produce *t*$BuNH_2$ and CO (Fig. 6A). Considering the similarity between isonitriles and nitriles, nitrile hydration is likely to proceed in a similar manner (Fig. 6B). When a nitrile coordinates to the metal, the nitrile carbon is attacked by a water molecule, activated by Oδ of αCys114-SO^-. The low k_{cat} value for isonitrile may be due to limited accessibility of the activated water molecule because of steric hindrance by Oδ of αCys114-SO^-. Nitrile coordination to the Fe^{3+} was suggested by electron spin resonance measurements (30). Involvement of αCys114-SO^- in the catalytic reaction had been suggested by our previous studies using the inhibitor, 2-cyano-2-propyl hydroperoxide (13), specifically oxidizing αCys114-SO^- to Cys-SO_2^-, and the site-directed mutant NHases (31). Yano *et al*. (32) have extensively studied the N_2S_2(*t*BuNC)$_2$-type Co^{3+} model complexes with different sulfur oxidation states and concluded that sulfur oxidations promoted the Lewis acidity of the Co^{3+} center and that only the sulfenyl oxygen exhibited a nucleophilic character. Theoretical calculation studies have indicated that Oδ of αCys114-SO^- could be a catalytic base when nitrile-coordination was assumed (19). These antecedent studies support the mechanism of the substrate coordinated to the iron being attacked by water activated by αCys114-SO^-. Recently, involvement of the Ser ligand (αSer112; corresponding to αSer113 of *Re*NHase) and of the vicinal Tyr and Trp residues (βTyr68 and βTrp72; corresponding to βTyr72 and βTyr76 of *Re*NHase) in the catalytic mechanism was suggested by temperature- and pH-dependent kinetic studies of the Co-type NHase from *Pseudonocardia thermophila* JCM 3095 (33). However, the corresponding residues of *Re*NHase were unchanged during our investigations (Fig. 4). Our findings represent the first structural evidence of reaction intermediates in NHase catalysis. The present results demonstrate a reaction mechanism in which the sulfenate group of αCys114-SO^- plays a key role in the catalysis. Cysteine oxidation has been found to play important roles in various proteins (34). The present work reveals a novel role of Cys-SOH as a catalytic base.

REFERENCES

1. Kobayashi, M., and Shimizu, S. (1998) *Nat. Biotechnol.* **16**, 733-736
2. Endo, I., Nojiri, M., Tsujimura, M., Nakasako, M., Nagashima, S., Yohda, M., and Odaka, M. (2001) *J. Inorg. Biochem.* ***83***, 247-253
3. Noguchi, T., Hoshino, M., Tsujimura, M., Odaka, M., Inoue, Y., and Endo, I. (1996) *Biochemistry* **35,** 16777-16781
4. Odaka, M., Fujii, K., Hoshino, M., Noguchi, T., Tsujimura, M., Nagashima, S., Yohda, M., Nagamune, T., Inoue, Y., and Endo, I. (1997) *J. Am. Chem. Soc.* **119,** 3785-3791
5. Bonnet, D., Artaud, I., Moali, C., Petre, D., and Mansuy, D. (1997) *FEBS Lett.* **409,** 216-220
6. Huang, W., Jia, J., Cummings, J., Nelson, M., Schneider, G., and Lindqvist, Y. (1997) *Structure* **5**, 691-699
7. Nagashima, S, Nakasako, M, Dohmae, N, Tsujimura, M, Takio, K, Odaka, M, Yohda, M, Kamiya, N, and Endo, I. (1998) *Nat. Struct. Biol*. **5**, 347-351
8. Miyanaga, A., Fushinobu, S., Ito, K., and Wakagi, T. (2001) *Biochem. Biophys. Res. Commun.* **288**, 1169-1174
9. Hourai, S., Miki, M., Takashima, Y., Mitsuda, S., and Yanagi, K. (2003) *Biochem. Biophys. Res. Commun.* **312**, 340-345
10. Arakawa, T., Kawano, Y., Kataoka, S., Katayama, Y., Kamiya, N., Yohda, M., and Odaka, M. (2007) *J. Mol. Biol.* **366**, 1497-1509
11. Noguchi, T., Nojiri, M., Takei, K., Odaka M., and Kamiya, N. (2003) *Biochemistry* **42**, 11642-11650 (2003).
12. Murakami, T., Nojiri, M., Nakayama, H., Odaka, M., Yohda, M., Dohmae, N., Takio, K., Nagamune, T., and Endo, I. (2000) *Protein Sci.* **9**, 1024-1030
13. Tsujimura, M., Odaka, M., Nakayama, H., Dohmae, N., Koshino, H., Asami, T., Hoshino, M., Takio, K., Yoshida, S., Maeda, M., and Endo, I. (2003) *J. Am. Chem. Soc.* **125**, 11532-11538
14. Shearer, J., Kung, I.Y., Lovell, S., Kaminsky, W., and Kovacs, J.A. (2001) *J. Am. Chem. Soc.* **123**, 463-468
15. Lugo-Mas, P., Dey, A., Xu, L.K., Davin, S.D., Benedict, J., Kaminsky, W., Hodgson, K.O., Hedman, B., Solomon, E.I., and Kovacs, J.A. (2006) *J. Am. Chem., Soc.* **128**, 11211-11221
16. Noverson, J.C., Olmstead, M.M., and Mascharak, P.K. (1999) *J. Am. Chem. Soc.* **121**, 3553-3554

17. Tyler, L.A., Noverson, J.C., Olmstead, M.M., and Mascharak, P.K. (2003) *Inorg. Chem.* **42**, 5751-5761
18. Heinrich, L., Mary-Verla, A., Li, Y., Vassermann, J., and Chottard, J. C. (2001) *Eur. J. Inorg. Chem.* **9**, 2203-2206
19. Hopmann, K.H., Guo, J.D., and Himo, F. (2007) *Inorg. Chem.* **46**, 4850-4856.
20. Hopmann, K.H., and Himo, F. (2008) *Eur. J. Inorg. Chem.*, **2008**, 1406–1412
21. Kubiak, K., and Nowak, W. (2008) *Biophys J.* (2008) **94**, 3824-3838
22. Taniguchi, K., Murata, K., Murakami, Y., Takahashi, S., Nakamura, T., Hashimoto, K., Koshino, K., Dohmae, N., Yohda, M., Hirose, T., Maeda, M., and Odaka, M. *J. Bioeng. Biosci.*, in press
23. Tsujimura, M., Odaka, M., Nagashima, S., Yohda, M., and Endo, I. (1996) *J. Biochem.(Tokyo)* **119**, 407-413
24. Otowinowski, Z., and Minor, W. (1997) *Methods Enzymol*. **276**, 307-326
25. Vagin A., and Teplyakov A. (1997) *J. Appl. Cryst*. **30**, 1022-1024
26. CCP4 (Collaborative Computational Project, Number 4). (1994) *Acta Crystallogr. Sect. D* **50**, 760-763
27. Murshudov, G.N., Vargin, A.A., and Dodson, E.J. (1997) *Acta Crystallogr. Sect. D*
28. Emsley, P., and Cowtan, K. (2004) *Acta Crystallogr. Sect. D.*, **60**, 2126-2132
29. Read, R. J. (1986) *Acta Crystallogr. Sect. A* **42**, 140-149
30. Sugiura, Y., Kuwahara, J., Nagasawa, T., and Yamada, H. (1987) *J. Am. Chem. Soc.* **109,** 5848-5850
31. Takarada, H., Kawano, Y., Hashimoto, K., Nakayama, H., Ueda, S., Yohda, M., Kamiya, N., Dohmae, N., Maeda, M., and Odaka, M. (2006) *Biosci. Biotechnol. Biochem*. **70**, 881-889
32. Yano, T., Wasada-Tsutsui, Y., Arii, H., Yamaguchi, S., Funahashi, Y., Ozawa, T., and Masuda, H. (2007) *Inorg. Chem.* **46**, 10345-10353
33. Mitra, S., and Holz, R.C. (2007) *J. Biol. Chem.* **282**, 7397-7404
34. Claiborne, A, Mallett, T.C., Yeh, J.I., Luba, J., and Parsonage, D. (2001) *Adv. Protein Chem.* **58**, 215-276

FOOTNOTES

*We are grateful to beamline assistants of the Photon Factory (PF) for data collection at beamline BL-5A. We thank Drs. K. Noguchi and A. Ohtaki of Tokyo University of Agriculture and Technology and Prof. N. Kamiya of Osaka City University and Dr. M. Nojiri of Osaka University for useful advice

and discussion on the structural determination and analyses of the intermediate structure of NHase. We also thank Prof. K. Nagasawa and Mr. M. Tera of Tokyo University of Agriculture and Technology and Prof. T. Ozawa of Nagoya Institute of Technology for fruitful discussion on the catalytic mechanism. This work was financially supported partly by a Grant-in-aid for scientific research from the "Future nano materials" section of the "21st Century Center of Excellence (COE)" project, a Grant-in-Aid for Scientific Research (B) (KAKENHI 19350080) (to M. O.), a Grant-in-Aid for Creative Scientific Research (17GS0314) (to T. N.), a Grant-in-Aid for JSPS Fellows (19252) (to H. S.) from the Japanese Society for the Promotion of Science (JSPS), and a grant of the National Project on Protein Structural and Functional Analyses from the Ministry of Education, Science, Sports and Culture of Japan (to M. Y.). This work was performed with the approval of the Photon Factory Advisory Committee (approval No. 2006G392).

The abbreviations used are as follows: NHase, nitrile hydratase; *Re*NHase, nitrile hydratase from *Rhodococcus erythropolis* N771; Cys-SO_2H, cysteine sulfinic acid; Cys-SOH, cysteine sulfenic acid; *t*BuNC, *tert*-butylisonitrile; *t*BuNH_2, *tert*-butylamine; ATR-FTIR, attenuated total reflectance-Fourier transform infrared; NO, nitric oxide; CO, carbon monoxide.

The atomic coordinates and structure factors for *Re*NHase in the nitrosylated state without and with *t*BuNC, and for *Re*NHase with *t*BuNC after light illumination for 18, 120, 340 and 440 mins, have been deposited in the Protein Data Bank with accession codes 2ZPB, 2ZPE, 2ZPF, 2ZPG, 2ZPH and 2ZPI, respectively.

FIGURE LEGENDS

Fig. 1. The sample unit of the ATR-FTIR measurement for CO detection using hemoglobin. Hemoglobin was loaded on a Si ATR prism, and an NHase solution and *t*BuNC were separately placed in a sealed space. *t*BuNC was supplied to the NHase solution as a vapor, and the reaction was initiated by photoactivation of NHase.

Fig. 2. ATR-FTIR difference spectra showing product formation by the NHase reaction with *t*BuNC. FTIR spectra of **(A)** $H_2{}^{16}O$ and **(B)** $H_2{}^{18}O$ solutions including NHase and *t*BuNC were recorded before and 100 (purple), 300 (blue), 500 (cyan), 700 (green) and 900 (red) s after illumination of *Re*NHase, and difference spectra were calculated relative to before illumination values. **(C)** The

spectrum of *tert*-butylamine (*t*BuNH$_2$) in an aqueous solution (in a protonated *t*BuNH$_3^+$ form) after subtraction of water absorption is presented for comparison.

Fig. 3. The CO-stretching region of the ATR-FTIR spectra of hemoglobin. Hemoglobin was loaded on an Si ATR prism, and NHase in an **(A)** $H_2{}^{16}O$ or **(B)** $H_2{}^{18}O$ buffer and *t*BuNC were separately placed in a sealed space (Fig. 2). Spectra at 0 (blue), 20 (cyan), 30 (green) and 60 (red) min after photoactivation of NHase were recorded.

Fig. 4. Structures around the non-heme Fe^{3+} center of *Re*NHase. F_o-F_c electron densities (3.0 σ contour as green and -3.0 σ contour as red) superimposed on the refined structures. NO and *t*BuNC molecules and Sγ of βMet40 were excluded from the calculation. **(A)** Nitrosylated NHase before soaking, **(B)** nitrosylated NHase with *t*BuNC, **(C)-(E)** NHase with *t*BuNC after light illumination for **(C)** 18, **(D)** 120 and **(E)** 440 mins. **(F)** F_o-F_c electron density (3.0 σ contour as green and -3.0 σ contour as red) and $2F_o$-F_c electron density (1.0 σ contour as gray) superimposed on the refined structure at 440 min. *t*BuNH$_2$ was included in the calculation. αCSD112 and αCSO114 indicate αCys112-SO_2^- and αCys114-SO^-, respectively. Yellow, blue, red, green and brown spheres represent carbon, nitrogen, oxygen, sulfur and iron atoms, respectively.

Fig. 5. The steric hindrance at Sγ of βMet40 caused by *t*BuNC. The refined structure around βMet40 in the nitrosylated NHase **(A)** without and **(B)** with *t*BuNC. Yellow, blue, red and green spheres represent carbon, nitrogen, oxygen and sulfur atoms, respectively. The black and red dashed lines indicate the distances between Sγ of βMet40 and the isonitrile carbon, and between Sγ of βMet40 and the amide oxygen of βMet40.

Fig. 6. Proposed catalytic mechanisms of NHase**. (A)** Isonitrile hydrolysis and **(B)** nitrile hydration.

Table 1. Data collection and refinement statistics

	Nitriosylated NHase[a]	0min[a,b]	18min[a]	120min[a]	340min[a]	440min[a]
Data collection						
Space group	*C2*	*C2*	*C2*	*C2*	*C2*	*C2*
Cell dimensions						
a, *b*, *c* (Å)	114.7, 60.5, 81.9	114.0, 60.0, 81.7	114.0, 60.0, 81.7	114.1, 60.1, 81.7	113.9, 60.2, 81.4	114.0, 60.2, 81.5
α, β, γ (°)	125.0	125.1	125.1	125.1	125.1	125.1
Wavelength (Å)	1.00000	1.00000	1.00000	1.00000	1.00000	1.00000
Resolution (Å)	50.0-1.30 (1.35-1.30)[c]	50.0-1.48 (1.53-1.48)[c]	50.0-1.48 (1.53-1.48)[c]	50.0-1.39 (1.44-1.39)[c]	50.0-1.59 (1.65-1.59)[c]	50.0-1.49 (1.54-1.49)[c]
R_{merge}	0.051 (0.293)	0.035 (0.118)	0.038 (0.108)	0.038 (0.271)	0.036 (0.208)	0.042 (0.216)
$I / \sigma I$	24.4 (3.49)	26.8 (10.5)	26.1 (10.8)	24.1 (3.71)	27.9 (4.04)	24.4 (3.97)
Completeness (%)	98.8 (97.2)	98.3 (93.6)	97.0 (93.1)	98.0 (90.2)	97.3 (85.3)	93.8 (75.9)
Redundancy	3.7	2.1	2.0	1.8	1.8	1.9
Refinement						
Resolution (Å)	7.96-1.30	8.00-1.48	8.00-1.48	7.98-1.39	7.99-1.59	8.00-1.49
No. reflections	105,634	69,876	68,831	84,855	55,536	65,146
R_{work} / R_{free}	16.9/18.7	16.8/19.4	16.8/19.0	17.7/20.1	15.8/18.5	15.9/18.3
No. atoms						
Protein	3,288	3,252	3,255	3,222	3,185	3,185
Ligand/ion	4	5	5	5	12	13
Water	756	663	643	601	538	545
B-factors						
Protein	11.7	13.4	14.1	14.5	11.2	11.7
Ligand/ion	18.7	16.6	20.9	29.8	18.6	20.4
Water	28.8	28.3	29.1	20.7	27.2	28.6
R. m. s. deviations						
Bond length (Å)	0.007	0.008	0.008	0.007	0.009	0.007
Bond angles (°)	1.151	1.198	1.188	1.184	1.184	1.160
Ramachandran plot						
most-favored (%)	98.5	98.0	98.2	98.5	98.2	98.2
additionally allowed region (%)	1.5	2.0	1.8	1.5	1.8	1.8

[a]One crystal was used to collect the data of each complex. [b]"0min" represents nitrosylated NHase soaked with *t*BuNC. [c]Highest resolution shell is shown in parenthesis.

Table 2. Selected bond lengths for the complex of nitrosylated NHase with *t*BuNC after light irradiation for 440 min.

	Bond lengths [Å]				
Fe-C(-NC)	2.1	C(-NC)-N(-NC)	1.4	C(-NC)-O(H_2Oa)	2.3
				N(-NC)-O(H_2Oa)	1.8
				O(SO)-O(H_2Oa)	1.6

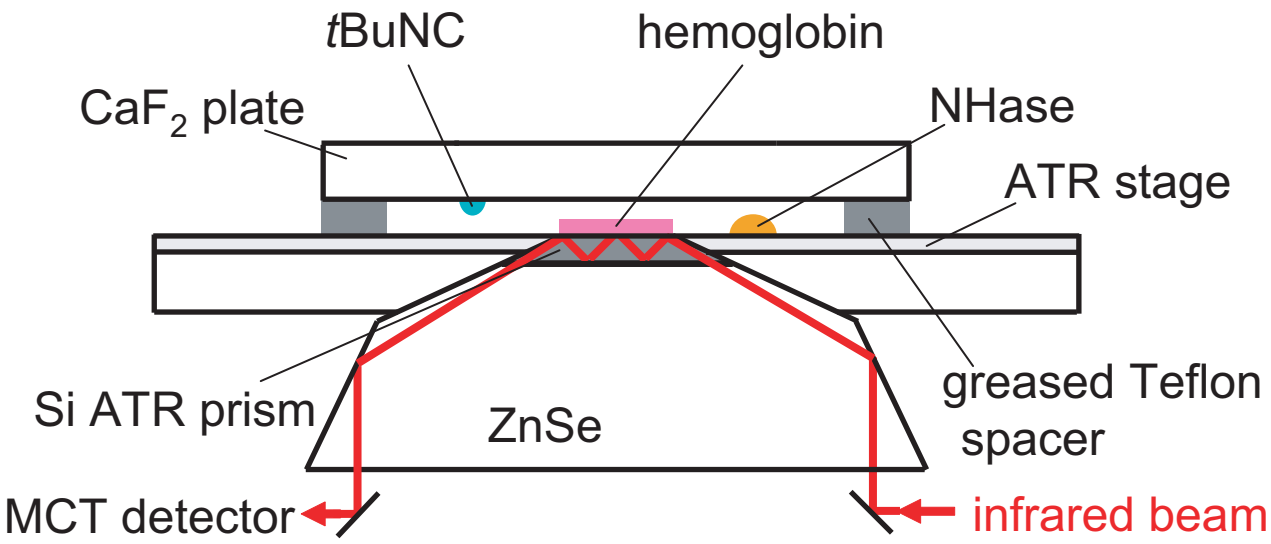

Hashimoto et al., Fig. 1

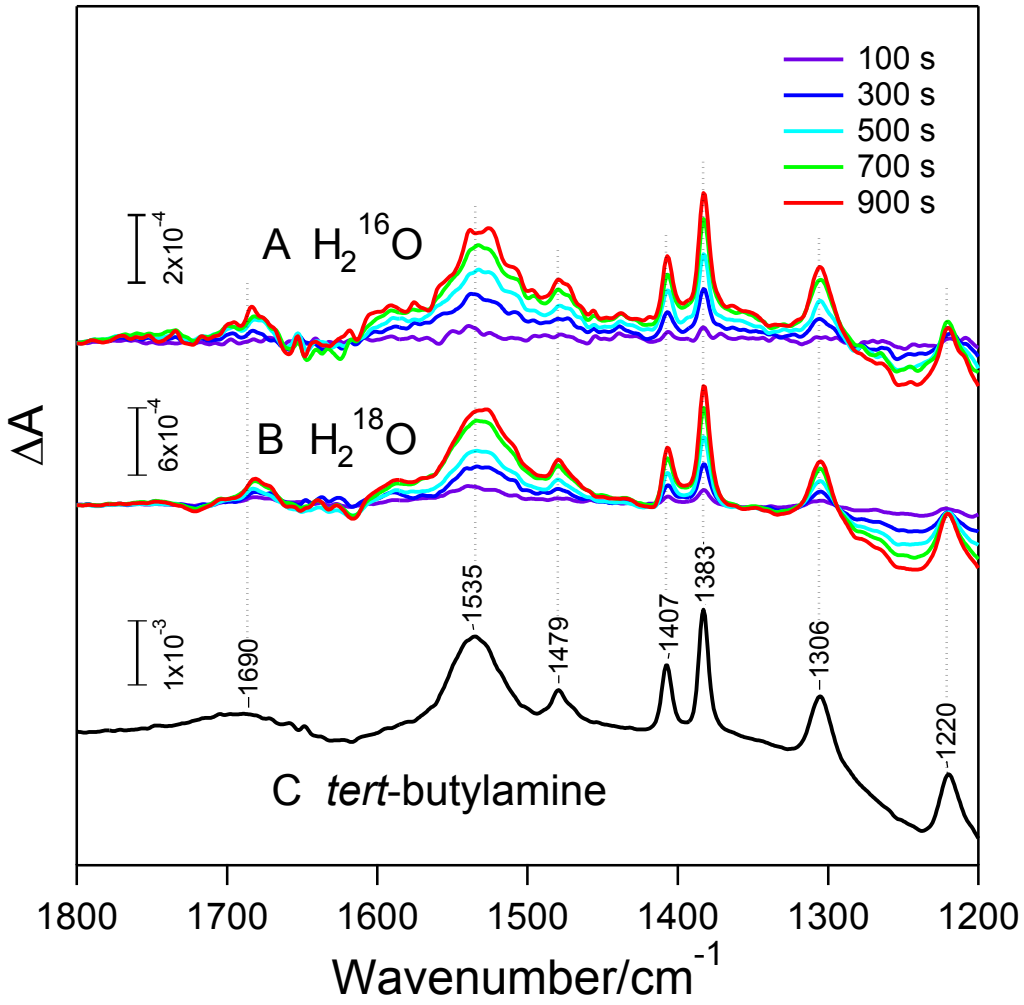

Hashimoto et al., Fig.2

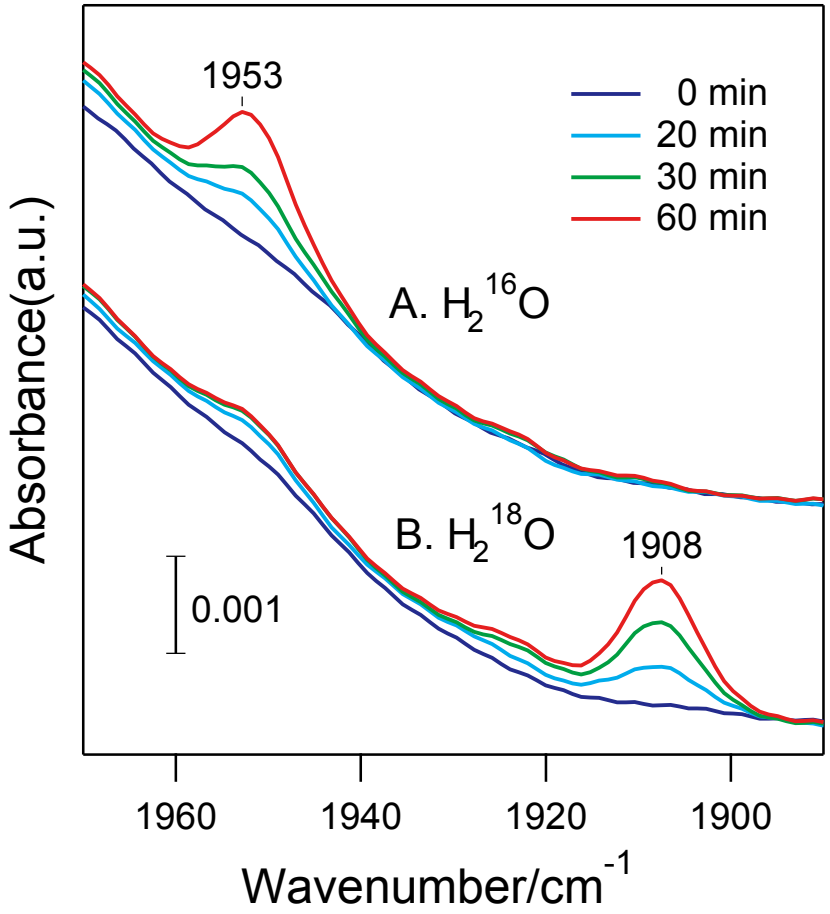

Hashimoto et al., Fig. 3

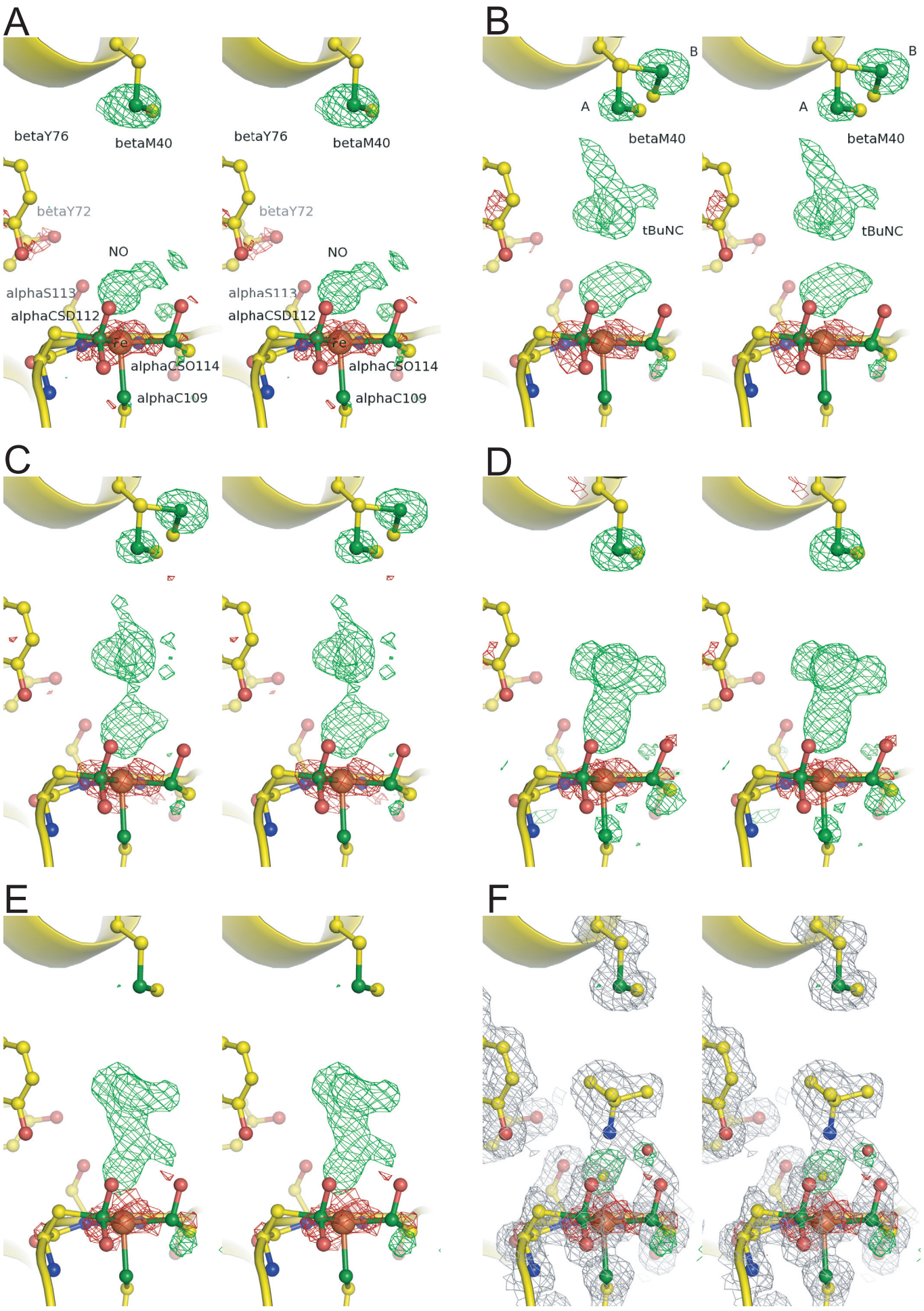

Hashimoto et al., Fig. 4

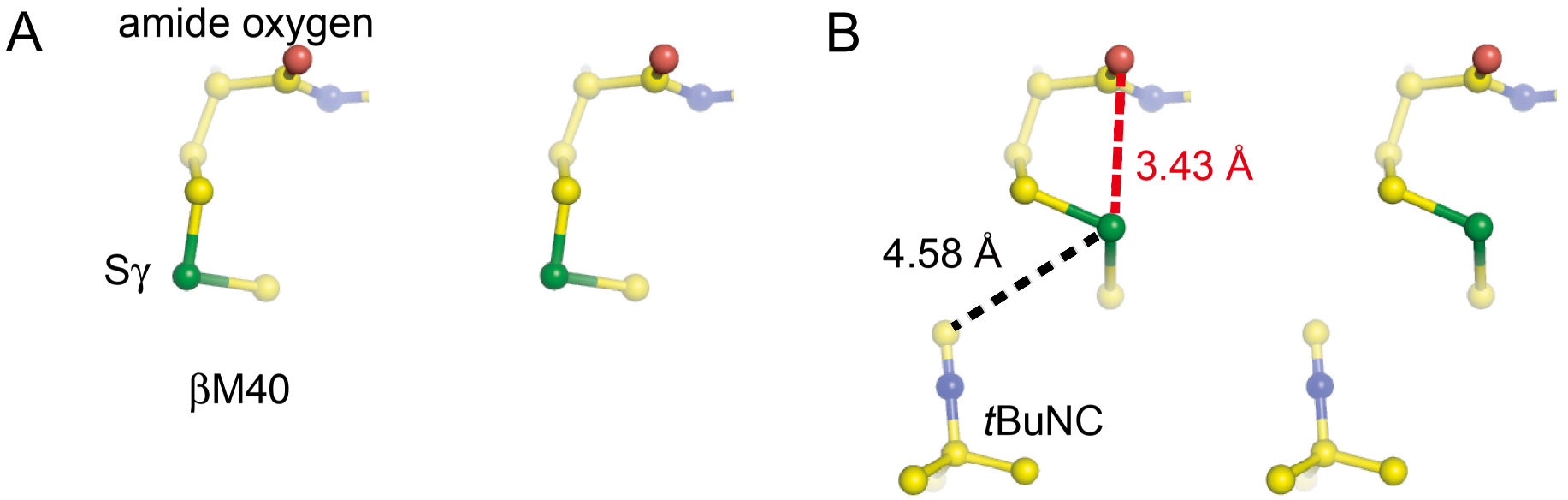
A
amide oxygen
Sγ
βM40
B
3.43 Å
4.58 Å
tBuNC

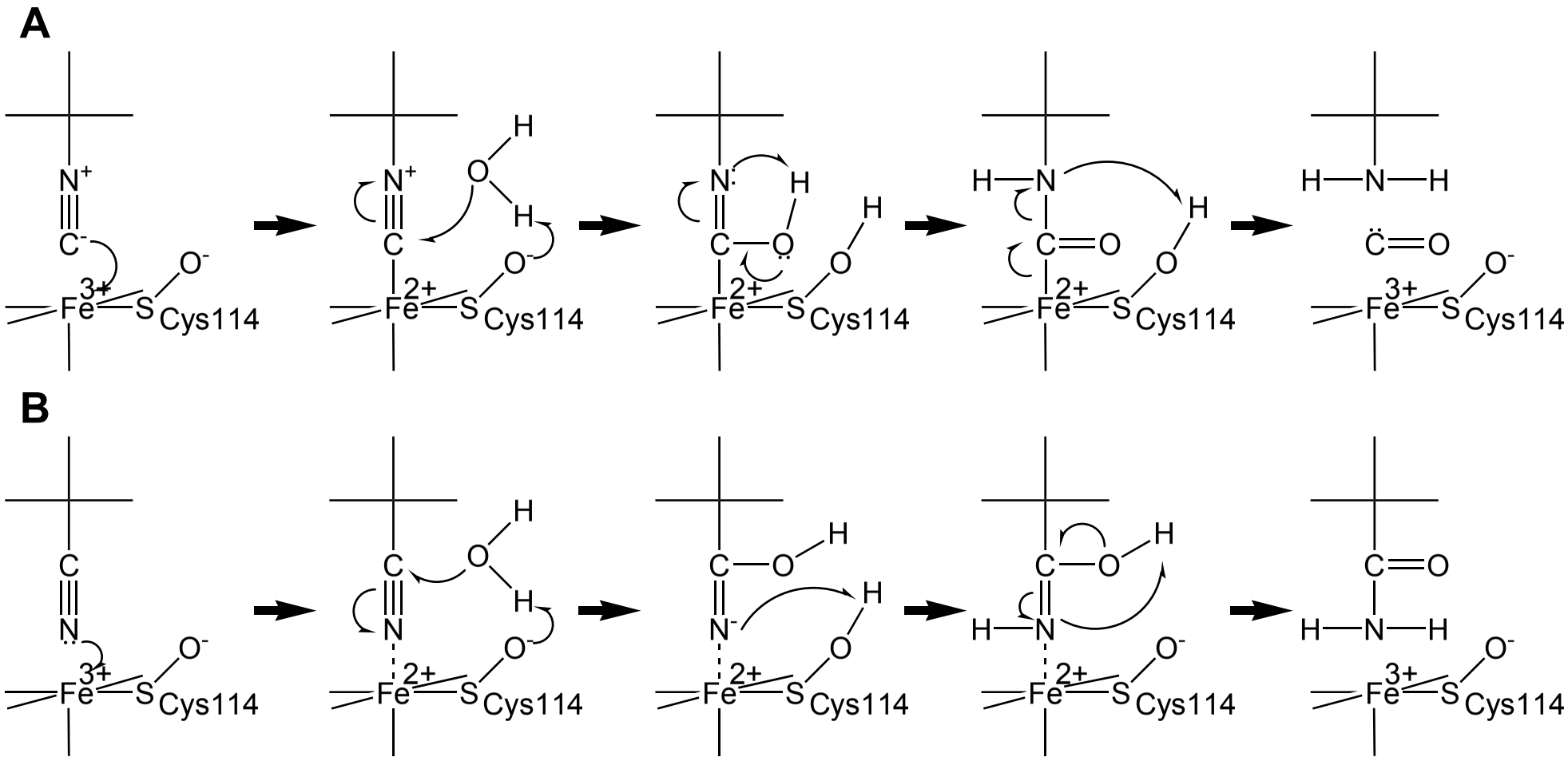

Hashimoto et al., Fig. 6